

Commissioning and Implementing a Quality Assurance Program for Dedicated Radiation Oncology MRI Scanners

Éric Poulin^{1,2}; Frederic Lacroix^{1,2}; Jean-David Jutras^{1,2}

¹Département de physique, de génie physique et d'optique et Centre de recherche sur le cancer de l'Université Laval, Université Laval, Québec, Canada

²Département de radio-oncologie et Axe Oncologie du Centre de recherche du CHU de Québec, CHU de Québec-Université Laval, Québec, Canada

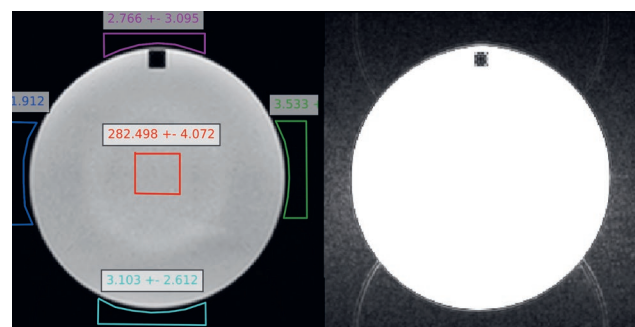
Introduction

Modern radiation oncology treatment, neuro navigation and intraoperative magnetic resonance imaging (MRI) require high geometric fidelity images in combination with high spatial and contrast resolution in order to precisely identify disease extent and adjacent organs at risk (OAR). Magnetic resonance imaging (MRI) has demonstrated superior soft tissue contrast and was shown to substantially improve target and OAR segmentation accuracy and reliability [1–4]. In addition, it was demonstrated that MRI can reduce treatment-related toxicities due to more accurately delineated OARs [5–7] and identify regions of high tumor burden to facilitate dose escalation [6, 8, 9]. However, conventional computed tomography (CT) simulation is still needed for many disease sites with target and OAR definition performed after MRI-to-CT image registration. This co-registration process may introduce geometrical uncertainties in the range of ~2 mm for the brain [10] and pelvis [11], and up to 5 mm in the abdomen [12] particularly if performed in a radiology setting. Furthermore, MR images are often used without considering the intrinsic geometric fidelity, precision and stability of the MR machine; an approach that may adversely impact dosimetric endpoints and increase the uncertainty beyond co-registration errors. For example, a recent radiosurgery study showed that geometric accuracy becomes a critical issue with small targets; for a target diameter of 3 cm, geometric distortions of 1.5 mm may impact the dose to 95% of the volume, while for targets less than 2 cm, a geometric distortion of 1 mm could significantly affect plan acceptance/quality indices [13].

A 2011 study showed a 78% failure rate during American College of Radiology (ACR) Quality Assurance testing [14]. The impact of geometric distortion in MR-guided radiation therapy has been the object of a recent study which demonstrated a relation between margin and system-related geometric distortion [15]. Neuronavigation accuracy was also shown to be affected by MRI geometric distortion [16]. Overall, the impact from

distortions will depend on factors such as the distance of the anatomy from the magnet isocenter, magnetic field strength, and MRI acquisition parameters and sequences, as well as MRI magnet and gradient coil properties. To address these limitations, dedicated MR simulator platforms have been recently introduced with the aim of improving the accuracy of target and OAR delineations required for radiotherapy treatment planning [17]. Moreover, the ACR [18] and American Association of Physicists in Medicine (AAPM) task group's [19–21] guidelines were recently published, addressing the specific aspects of a quality assurance program and commissioning for both cases of MR images used in conjunction with CT, as well as MR images used as a primary modality.

The radiation oncology department of the CHU de Québec-Université Laval is moving into a brand-new facility and accordingly acquired two new MRI machines dedicated to radiation therapy (RT) (MAGNETOM Aera and MAGNETOM Sola, Siemens Healthcare, Erlangen, Germany). The goal of the current paper is therefore to present the authors' experience regarding the commissioning and introduction of a Quality Assurance program for radiation oncology-dedicated MRI scanners.



1 Ghosting ratio test, showing ROI locations on a uniform slice of the ACR phantom.

Materials and Methods

MRI systems

The CHU de Québec – Université Laval acquired a MAGNETOM Sola 1.5T MRI simulator (Siemens Healthcare, Erlangen, Germany) dedicated to external-beam RT planning and a Nexaris MR with MAGNETOM Aera 1.5T scanner (Siemens Healthcare, Erlangen, Germany) for interventional brachytherapy. The MAGNETOM Sola is equipped with XQ gradients (45 mT/m, 200 T/m/s), a fixed table (for improved setup accuracy) and the *syngo* MR XA20 software platform with high-end computing (later upgraded to *syngo* MR XA31 on November 2021); it also has the complete QFix solution for radiotherapy simulation (QFix, Avondale, PA, USA) and the DORADOnova MR3T LAP laser system (LAP GmbH Laser Applikationen, Lüneburg, Germany). The Nexaris MR with MAGNETOM Aera is equipped with XQ gradients (45 mT/m, 200 T/m/s), a dockable table, an additional Combi-Suite Dockable Table and was installed with the *syngo* MR E11E software platform on March 2021 and later upgraded to *syngo* MR XA30 on September 2021.

Commissioning and QA

The development of wide bore (70 cm) high field (≥ 1.5 T) MRI scanners starting with the Siemens MAGNETOM Espree in 2004 has provided the within-bore space to image patients in Radiation Oncology treatment position and with dedicated immobilization devices in place. Recently, RT-dedicated MRI simulator platforms incorporating external lasers, a flat RT table, and specialized RT workflows have been made available by the major scanner manufacturers and are being installed in Radiation Oncology departments worldwide. The integration of dedicated MRI systems into the radiotherapy workflow necessitates the development of specific Quality Assurance programs as well as acceptance/commissioning tests. The AAPM as well as the Canadian Partnership for Quality Radiotherapy (CPQR) have drafted recommendations for the establishment of Quality Assurance (QA) programs [20–23] and commissioning [20, 22] for dedicated MRI RT systems. All mandatory commissioning tests suggested by the AAPM report 284 [22] were performed and the authors' main findings are shown in the results section. QA tests and associated tolerances are defined so as to ensure the highest possible geometric accuracy, image integrity and stability of RT MRI images. Table 1–4 summarizes the QA program established at the CHU de Québec, which is derived from the most recent AAPM and CPQR recommendations for RT MRI.

Table 1–4 provides an overview of the QA tests to be performed according to their frequency: daily, monthly, semi-annual and annual. Column 1 provides a short description of the test and column 2 outlines its associated analysis method. A variety of analysis methods are used:

visual inspection, in-house tools provided by the Siemens Healthineers clinical or service platform, third party software (e.g. AutoQApplus from QA Benchmark, Frederick, MD, USA, and GRADE QA software, Spectronics Medical, Helsingborg, Sweden) or in-house python-based code. Tests in Table 1 are performed by the radiation therapists but the MRI physicists do the ACR analysis. Most monthly, semi-annual and annual tests are performed by the MRI physicists, except for a few specific tests in Table 4 which may only be performed by a certified Siemens Healthineers technician, for example the emergency quench button check. A level 5 service key is necessary in order to run the Siemens Healthineers service platform tests while a level 7 service key is necessary to visualize the detailed results and export the analysis in a PDF file format.

In the QA program established at the CHU de Québec–Université Laval, the lasers are verified and adjusted using the Aquarius phantom from LAP (Lüneburg, Germany). Note that the MAGNETOM Aera scanner (dedicated to brachytherapy) has no external LAP laser system and no UltraFlex antennas. The Siemens Healthineers service phantoms, including a 25 cm sphere for B_0 homogeneity, and various cylindrical phantoms and custom-fitting foam mats for antenna channel uniformity testing are also used. The Siemens Healthineers service tests and platform were previously shown in a white paper [24] and the prescribed methodology was followed here; ACR testing is also shown.

The geometric accuracy of MR images has always been of paramount concern in RT. Geometric distortions in MR images arise from two main sources:

- 1) system-related effects and
- 2) patient-related effects.

System-related effects include the B_0 field inhomogeneity and the gradient nonlinearities. Patient-related effects include magnetic field susceptibility variations in the body of the patient, while the chemical-shift artifact is both a system and patient-related effect. The resulting total distortion is highly dependent on the imaging parameters including the specific pulse sequence, acquisition orientation, the field-of-view (FOV), acquisition and RF pulse bandwidth (BW), as well as being patient-dependant. It has been shown that system-related distortions typically are greater than patient-related distortions and that gradient nonlinearities can be the largest-contributing source of geometric distortions [25]. While the patient-specific distortions are more difficult to mitigate, vendors have incorporated two dimensional (2D) or three dimensional (3D) algorithms to automatically correct raw MRI data for known gradient nonlinearities. Such algorithms, however, do not correct for B_0 inhomogeneity and suffer from residual distortion. It has been demonstrated that the residual distortions once vendor-supplied 3D correction factors are applied, can be greater than 1 mm at 10 cm from the isocenter [22]. An accurate characterization of

| Daily QA | |
|--|---------------------------|
| Test | Analysis Method |
| Safety and emergency (cameras, intercom, emergency buttons, O ₂ sensor) | Visual |
| Mechanical QA (table, antenna and connector integrity, temperature, helium, water level) | Visual |
| ACR phantom with alternate daily coil setup (Monday-Friday) | QA Benchmark software |
| Image origin correspondence with LAP lasers (Sagittal localizer sequence on ACR) | Siemens clinical platform |
| Transmit gain setting (T1w SE sequence on ACR) | Siemens clinical platform |
| SNR stability (T1w SE sequence on ACR) | Siemens clinical platform |

Table 1: MRI Daily Quality Assurance tests performed as part of a Radiation Therapy QA program.

| Monthly QA | |
|---|---|
| Test | Analysis Method |
| Coil QA (for all regularly-used coils e.g. Body-18, Body-30, Head&Neck-20, UltraFlexLarge-18, Spine-32) | Siemens service platform |
| RF noise check | Siemens service platform |
| RF spike check | Siemens service platform |
| B ₀ homogeneity phantom shim check | Siemens service platform / Siemens customer platform ¹ |
| Helium level and cooling water flow rate | Siemens service platform |
| RF artifact check (based on the ACR image data of the month) | Visual |
| 3D geometric distortion QA with gradient correction using 3DGRADE phantom (gre_ax_LR only) | Spectronics software |
| EPI average ghosting ratio check (on ACR phantom) | In-house python code |
| EPI geometric distortion check (on ACR phantom) | In-house python code |
| EPI long-term stability check (on ACR phantom) | In-house python code |

Table 2: MRI Monthly Quality Assurance tests performed as part of a Radiation Therapy QA program.

¹These QA tests are available on the Siemens Healthineers customer platform with MAGNETOM Sola and Vida scanners on syngo MR XA31 software and later versions, only. Otherwise, the tests are available on the Siemens Healthineers service platform.

| Semi-Annual QA | |
|--|---|
| Test | Analysis Method |
| Gradient eddy-currents compensation/cross-term check | Siemens service platform |
| Gradient sensitivity check | Siemens service platform / Siemens customer platform ¹ |
| Body coil tuning check | Siemens service platform |
| RF gain calibration check | Siemens service platform |
| Transmitter gain stability check | Siemens service platform |
| Slice position/thickness synthesizer check | Siemens service platform / Siemens customer platform ¹ |
| LAP Lasers-on-marks verification (laser location is marked on the walls/ceiling around the room) | Visual |
| Table semi-annual test using Aquarius phantom | Siemens clinical platform |

Table 3: MRI Semi-Annual Quality Assurance tests performed as part of a Radiation Therapy QA program.

| Annual QA | |
|---|--------------------------|
| Test | Analysis Method |
| Coil QA (for all other coils not verified monthly, e.g. FlexSmall-4) | Siemens service platform |
| B ₀ inhomogeneity check using dual-echo 3D GRE using the 25cm Siemens sphere of NiSO ₄ solution | In-house python code |
| 3D geometric distortion QA without gradient correction on 3DGRADE phantom (gre_ax_LR only) | Spectronics software |
| Parallel Imaging SNR verification on 3D MPRAGE for SRS (using ACR phantom) | In-house python code |
| B ₀ -field lines verification with Gauss meter incl. 5/200 Gauss | Visual |
| Mechanical table movement QA with ruler (5, 10, 20, 200, 350mm) | Visual |
| Secondary Systems check (incl. injector, anesthesia) | Visual |
| Oxygen sensor check | Visual |
| Electrical shutdown check | Siemens Technician |
| Table movement during emergency check | Siemens Technician |
| Quench button check | Siemens Technician |

Table 4: MRI Annual Quality Assurance tests performed as part of a Radiation Therapy QA program.

the system-related effects is therefore of paramount importance for the correct use of MR images in RT. This is especially critical in the event that MR images are not fused to planning CT images, but used in a standalone fashion for MR-only RT planning. Therefore, geometric distortions were tested using the GRADE QA phantom (Spectronic Medical SE, Karbingatan, Sweden). The GRADE QA phantom consists of approximately 1200 17 mm diameter spherical markers made of polyethylene glycol imbedded in expanded foam [26]. The resulting phantom is of large diameter (47.9 cm lateral, 38.5 cm height and 50 cm longitudinal) and relatively light weight (approximately 10 kg). Note that the MAGNETOM Sola FOV is $50 \times 50 \times 50 \text{ cm}^3$ while the MAGNETOM Aera FOV is slightly shorter in the longitudinal dimension and covers $50 \times 50 \times 45 \text{ cm}^3$. It is important to note that a significant portion of the FOV, namely the area located under the imaging table, is a “dead zone” with respect to MR imaging. The width, height and length of the GRADE QA phantom ensures that a significant proportion (> 90%) of the usable scanner FOV can therefore be characterized for distortion. A 3D FLASH sequence was used to image the GRADE QA phantom as recommended [26]. The sequence parameters (*FLASH3D_geo*) are provided in Table 5. The phase encoding direction selected was the Left-Right (LR) direction.

The goal of this QA program is to ensure the best possible performance of RT MRI scanners, while optimizing or minimizing the QA time requirements. A significant effort was made to automate the data analysis as much as possible through the use of in-house or third-party software. Note also that QA data logging and storage is performed using QATrack+, an open source database for managing QA data [27]. Every test contains one or more measurement results that are uploaded in QATrack+ and monitored over time.

CHU de Quebec in-house experience

For five of the quality assurance tests recommended by the AAPM reports, or the CPQR, no dedicated commercial

software exists yet; therefore, we had to develop our own in-house python programs to perform an automatic analysis. The analysis of those five tests is described below:

EPI geometric distortions

For the EPI geometric distortion check (recommended in the AAPM Report 100 [20]), the same EPI pulse sequence is employed as for the ghosting ratio measurement and is shown in Table 5. An additional turbo spin echo (TSE) sequence with the same FOV, slice positions and acquisition/reconstruction matrix size (shown also in Table 5) is used as a geometric reference to measure the EPI distortion in both frequency-encode and phase-encode directions. The ITK Canny Edge Detection Filter was used to automatically detect the edges of both the TSE and the EPI image as shown in Figure 6 of the Results section. From the edge masks, the distances in the central row and column of the images are automatically subtracted, yielding a relative measure of distortion in the frequency and phase directions to an accuracy in the order of the image resolution (1 mm).

EPI ghosting ratio

The EPI average ghosting ratio is calculated using Eq. 1 within the central uniform slice of the ACR phantom. The main EPI sequence parameters used are listed in Table 5.

$$1 \quad \%GR = \left| \frac{(S_L + S_R) - (S_T + S_B)}{2S_C} \right| \times 100\%$$

Here, S_L , S_R , S_T , S_B and S_C are the average signal in the left-side, right-side, top, bottom and central ROI locations shown in Figure 1, respectively. The ROIs are drawn manually for a first time as shown in Figure 1, and then saved as masks which can be re-used indefinitely to improve the consistency or reproducibility over time. A threshold of 3% was chosen as the acceptable upper limit for ghosting.

| Sequence Name | $\alpha/TR/TE/TE_2$ | # Slices | FOV (freq×ph×sl) | Acq. Voxel Resolution | BW | TSE / EPI factor | Scan time |
|------------------------|---------------------|----------|---------------------|-----------------------|------|---------------------|-----------|
| | °/ms/ms/ms | | (mm) | (mm) | | | (min:sec) |
| FLASH3D_geo | 20/6.0/2.16/ – | 480 | 500×500×480 | 0.98×0.98×1.0 | 330 | – / – | 24:36 |
| EPI_ghost_geo | 90/4860/61/ – | 34 | 240×240×170 | 1.88×1.88×5.0 | 1260 | – / 128 | 0:6 |
| TSE_ghost_geo | 150/4860/59/ – | 34 | 240×240×170 | 1.88×1.88×5.0 | 465 | 17/ – | 1:24 |
| EPI_stability | 90/3370/40/ – | 32 | 260×260×159 | 4.06×4.06×4.0 | 1202 | – / 64 | 8:30 |
| FLASH3D_B ₀ | 20/22/9.53/19.06 | 128 | 280×280×282 | 2.19×2.19×2.2 | 540 | – / – | 9:25 |

Table 5: Sequences with important parameters used in the QA program.

EPI long-term stability

The EPI long-term stability check was based on two previous publications, including the Glover stability QA protocol (GSQAP) [28] and the ROI analysis of Weisskoff [29]. Both analyses were performed on the same uniform ACR phantom slice of the *EPI_stability* sequence with parameters listed in Table 5.

B₀-inhomogeneity mapping

Although the B₀-homogeneity phantom shim check on the Siemens Healthineers service platform (Siemens customer platform¹ as of *syngo* MR XA31 for MAGNETOM Vida and MAGNETOM Sola) is run on a monthly basis (see monthly QA listed in Table 2), we also implemented a common B₀-inhomogeneity mapping technique described in both the AAPM report 284 [22] and the AAPM Report 100 [20]. Only the body-coil was used as receiver to avoid phase inconsistencies across various multi-channel head coils. The other alternative is to perform phase-unwrapping on each coil of a multi-coil array separately, but poses more challenges than benefits. The *unwrap phase* algorithm as part of the *skimage.restoration* python toolkit was found sufficiently robust to perform 3D phase-unwrapping on the 25 cm Siemens Healthineers spherical phantom images of a double-echo spoiled gradient echo sequence (*FLASH3D_B₀*) listed in Table 5. The following equation is employed to measure the final field inhomogeneity in ppm:

$$(2) \quad \Delta B_0 [\text{ppm}] = \frac{\Delta \phi [\text{rad}] (42.576 \frac{\text{MHz}}{\text{T}})}{\gamma [\frac{\text{MHz}}{\text{T}}] \Delta TE [\text{s}] f_0 [\text{MHz}]} \times 10^6 \text{ ppm}$$

Here, $\Delta \phi = \phi_2 - \phi_1$ is the phase difference after unwrapping the phase ϕ_1 , ϕ_2 corresponding to each echo TE₁, TE₂ with difference $\Delta TE = TE_2 - TE_1$, f_0 is the Larmor frequency (in MHz) of the scanner, and γ is the proton gyromagnetic ratio.

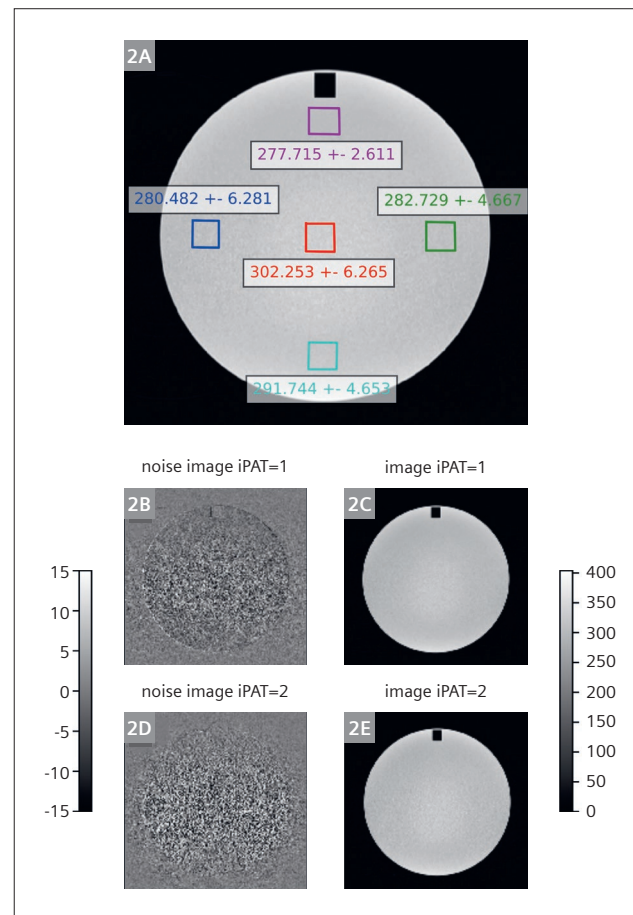
Parallel imaging SNR stability

The SNR verification of parallel imaging was performed using the image difference method (described in AAPM TG-118 [21]), via two 3D MPRAGE dynamics without acceleration ($R = 1$) and two with GRAPPA acceleration ($R = 2$), including 48 integrated k -space lines. The SNR ratios of $R = 1$ to $R = 2$ were then measured in five square ROIs inside the uniform slice of the ACR phantom image as shown in Figure 2. The 3D MPRAGE pulse sequence

with iPAT = 2 was the same as our in-house protocol optimized for brain stereotactic radiosurgery planning (FOV: 240 × 240 × 176 mm³, Acquisition matrix: 384 × 384, axial slice thickness 1 mm, reconstruction matrix: 768 × 768 × 176, TI/TR_{shot}/TR/TE/α = 845/1670/8.16/3.31 ms/10°, iPAT = 2 with 48 integrated lines, BW = 160 Hz/pixel, RL phase-encode direction, scan time: 6 min).

Evaluation of parallel imaging

Siemens Healthineers GRAPPA parallel imaging method allows the possibility to use an integrated or separated method to acquire the reference lines. The separated method uses a gradient echo (GRE) sequence and allows the user to choose the number of reference lines in both phase directions (in plane and slice). The impact of the reference line acquisition scheme on SNR and time was evaluated using the sequence and methodology described in the parallel imaging SNR stability test. The MPRAGE sequence was used and the acquisition time was recorded for each acquisition. For the integrated method, the number of lines was varied from 24 to 96 lines while for the GRE method



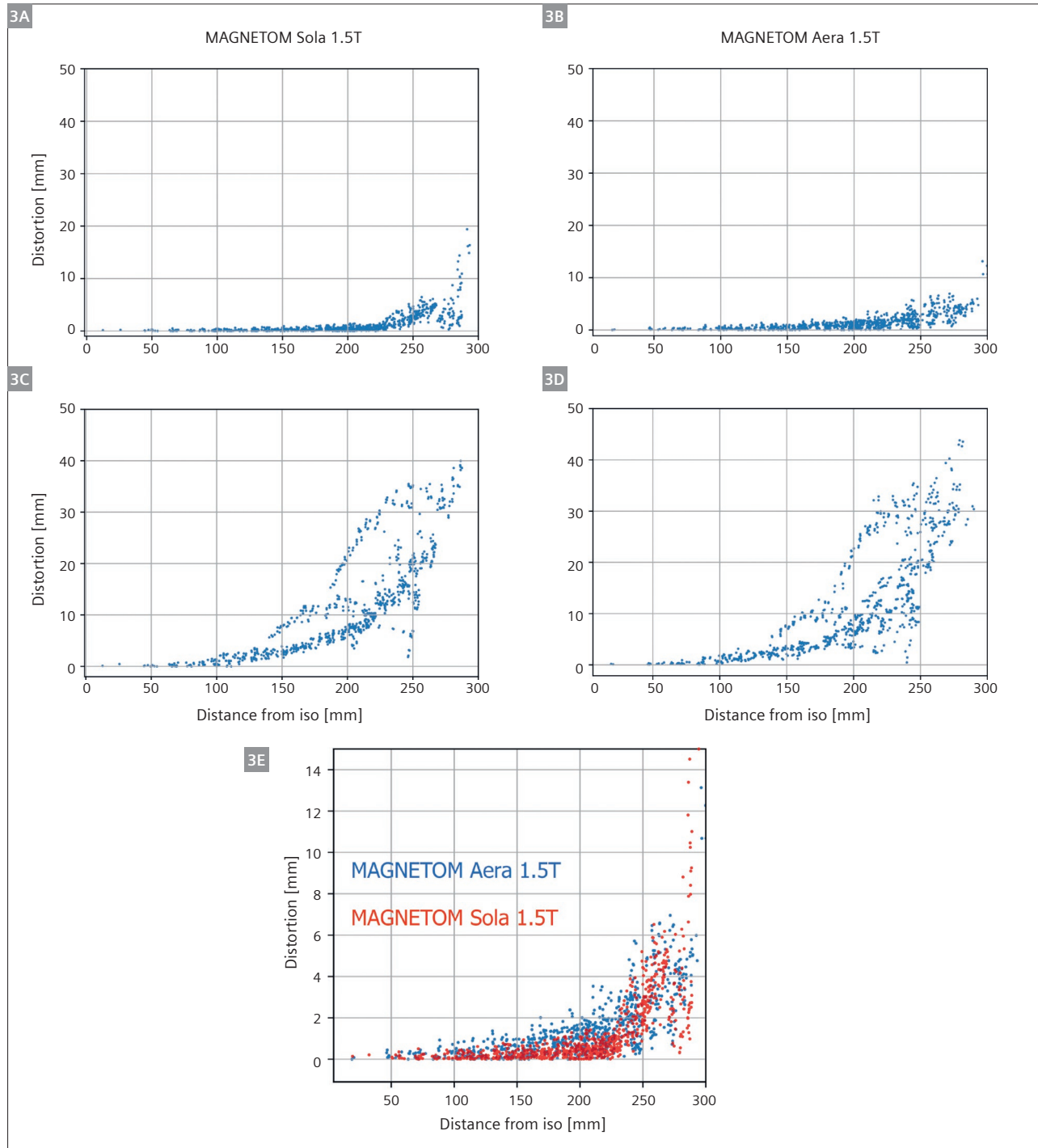
2 Parallel imaging SNR stability test showing (2A) ROI regions within the ACR phantom, (2B) noise image with iPAT = 1, (2C) image with iPAT = 1, (2D) noise image with iPAT = 2, (2E) image with iPAT = 2.

¹These QA tests are available on the Siemens Healthineers *MAGNETOM* World customer platform with *MAGNETOM* Sola and Vida scanners on *syngo* MR XA31 software and later versions, only. Otherwise, the tests are available on the Siemens Healthineers service platform.

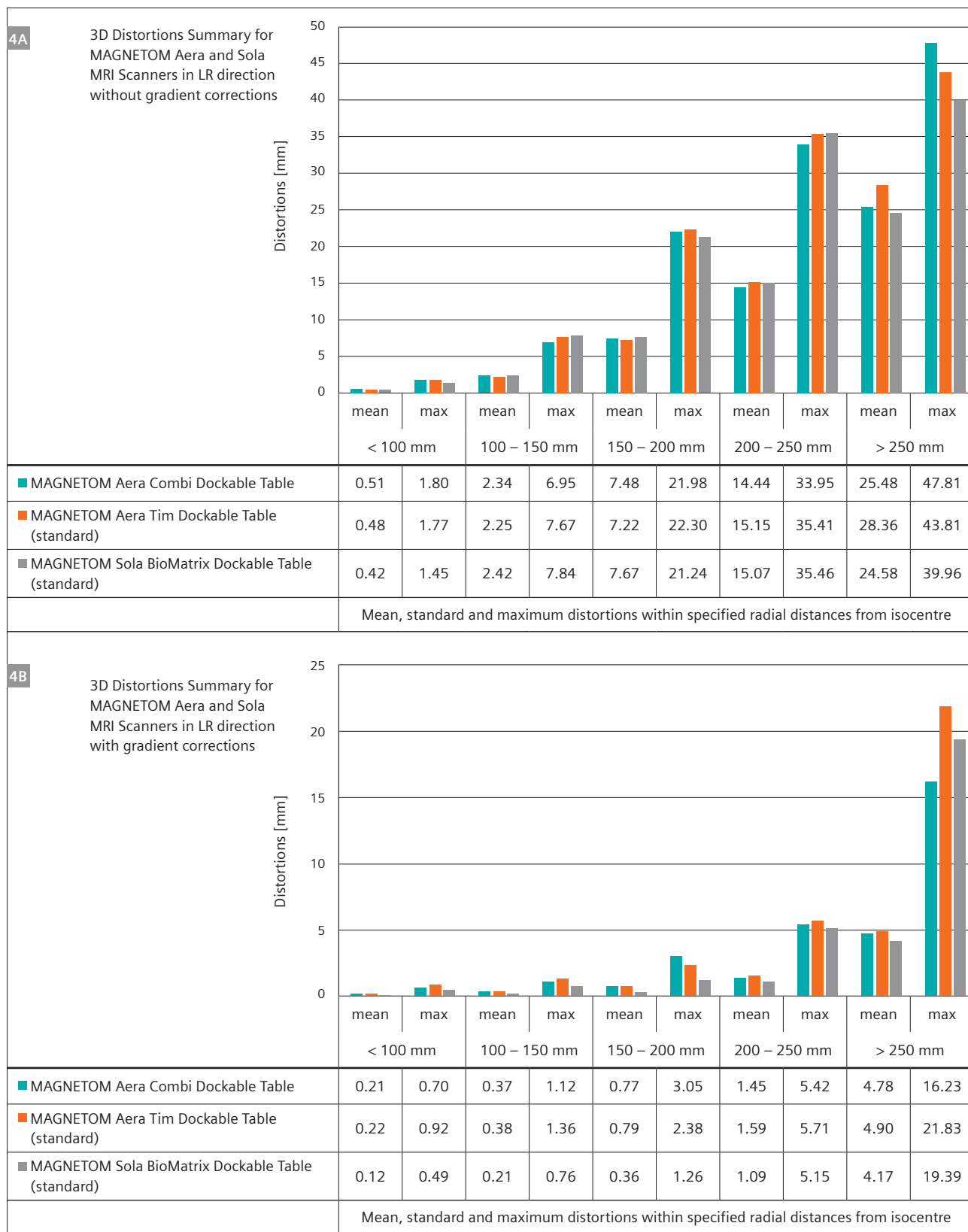
the following configurations were tested: 64 in-plane lines and 24 slice lines (gre 64-24) as well as 96 in-plane lines and 48 slice lines (gre 96-48).

Results

The complete AAPM TG 284, TG 100 and CPQR tests were performed as part of commissioning and no failures were detected on both MAGNETOM Aera and MAGNETOM Sola



3 Comparison of Siemens Healthineers MAGNETOM Sola (3A, C) vs MAGNETOM Aera (3B, D) distortion vector magnitude plots with (3A, B) and without (3C, D) gradient non-linearity correction (using the 3D GRADE phantom by Spectronics) for the LR phase-encode direction as a function of control point distance from the MRI isocentre. (3E) The gradient-corrected control point's distortions of both scanners are superposed on the same axes demonstrating significantly lower mean distortions in the MAGNETOM Sola compared to the MAGNETOM Aera scanner.



4 3D distortion mean and maximum values across spherical volumes of various radii from the imaging isocenter for the MAGNETOM Sola and MAGNETOM Aera scanners for the Left-Right (LR) phase encode direction without (**4A**) and with (**4B**) gradient corrections turned on for the standard and Combi Dockable Tables (MAGNETOM Aera only).

machines. One problem was found regarding coil QA; in fact SNR references were wrong for the Body-30 receiver coil and as a consequence the QA test kept failing; however this was corrected in version *syngo* MR XA31. Siemens Healthineers service platform allows for automatic QA processes (some QA processes are available on the Siemens Healthineers MAGNETOM World customer platform with MAGNETOM Sola and Vida scanners on *syngo* MR XA31 and later) which take less than an hour and these tests meet most of AAPM TG 284 and TG 100 recommendations. The service or customer QA platform allowed us to perform semi-automatic coil tests based on TG 284 recommendations. The time needed for testing depends on the coil itself (mainly dependant on the number of channels and length), but can range from 5 minutes to more than 20 minutes (e.g. spine-32 array or Body-30). Low-SAR RF pulses (the default setting in some sequences) were found to cause the ACR slice selection thickness test to fail with a value of 6.1 ± 0.2 mm, which was outside the tolerance of 5.0 ± 0.7 mm. The shim and gradient sensitivity had to be re-tuned during the first 9 months of operation for both machines, as well as Body Coil tuning for the MAGNETOM Sola. The shim-tuning was needed within the first 2 months post-commissioning and ramping up of the magnet.

Distortion characterization

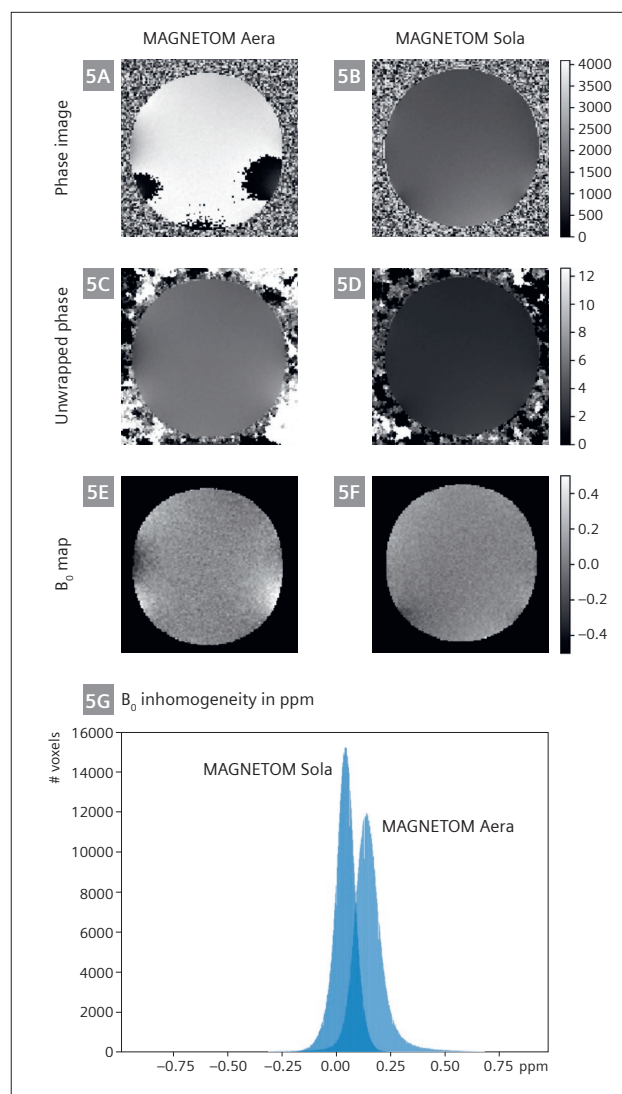
Figure 3 presents the raw, uncorrected (3A, 3B) and 3D corrected (3C, 3D) distortion vector magnitude plots as a function of the distance from the MRI isocenter for the MAGNETOM Sola and MAGNETOM Aera platforms. Figure 3E compares the 3D distortion for the MAGNETOM Sola and MAGNETOM Aera with gradient corrections turned on. Panels 3A, 3C and 3B, 3D of Figure 3 illustrate that applying the vendor-supplied gradient correction mitigates, to a large extent, the residual 3D distortion. For a radius of 250 mm, the residual 3D distortion is 35 mm without gradient correction, which reduces to 5 mm with the 3D distortion correction applied. Panel 3E shows that there is a tendency for lower average residual distortion on the MAGNETOM Sola as compared to the MAGNETOM Aera.

Figure 4 presents the mean and maximum 3D distortion values for different radii spheres centered around the imaging isocenter for the MAGNETOM Sola and MAGNETOM Aera scanners. In fact, it first illustrates the large effect of turning the 3D gradient corrections "On". The main effect is a halving, or more, of the mean and maximum residual distortion across the scanner field-of-view. On the MAGNETOM Sola, the average distortion is on the order of 1 mm for imaging radii of 250 mm or less. For radii of up to 200 mm, the maximum distortion is 1.26 mm and the average is 0.36 mm. Distortion values on the MAGNETOM Aera standard table are roughly double

the MAGNETOM Sola values for radii up to 200 mm. Distortion values for the Combi-Suite Dockable Table on the MAGNETOM Aera are comparable to values for the standard table.

B_0 inhomogeneity

Results of the B_0 inhomogeneity mapping in the 25 cm sphere for the MAGNETOM Aera and the MAGNETOM Sola 1.5T scanners are compared in Figure 5 in a sagittal slice. Note that the mean of the unwrapped phase (in 5C and 5D) can be close to any multiple of 2π , which explains the different intensities.



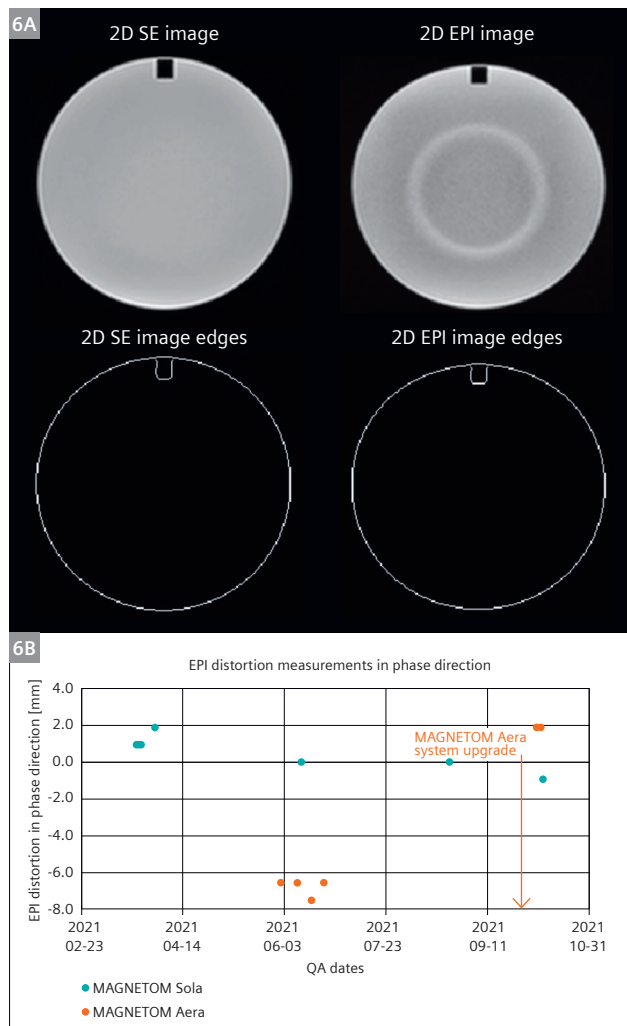
5 B_0 homogeneity test showing (5A) wrapped phase image, (5C) unwrapped phase image, (5E) B_0 inhomogeneity map in ppm for the MAGNETOM Aera system while (5B), (5D) and (5F) are equivalent for the MAGNETOM Sola system. Sub-figure (5G) is showing the histogram of the inhomogeneity superposed for both systems.

Advanced imaging

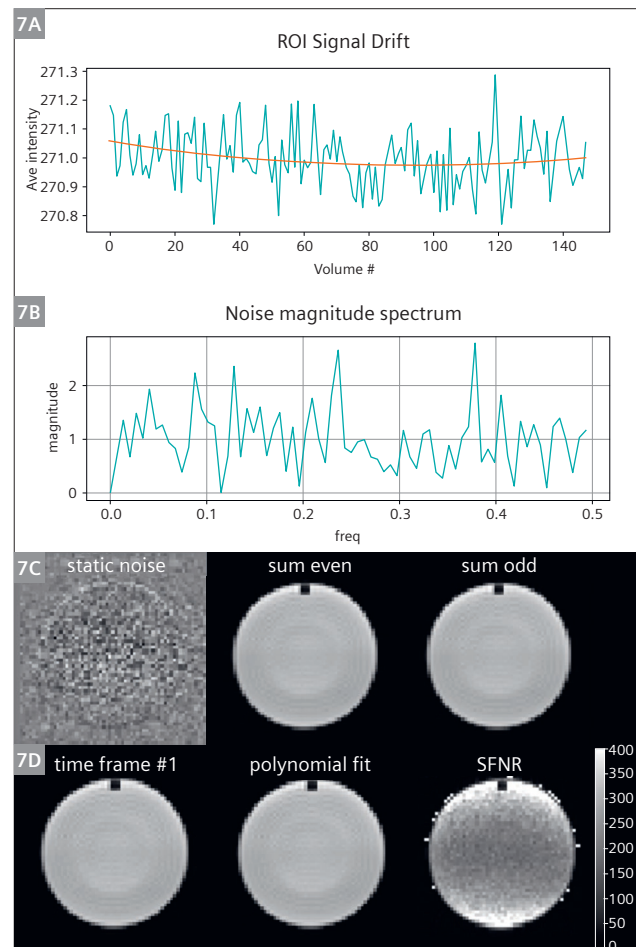
Figure 6 shows some phantom images and edge detection results from our automated EPI geometric distortions measurement. The distortion in the phase encoding direction in (6B) is shown for both scanners over a period of about 6 months. The range of EPI distortion was between 0 and 2 mm for the MAGNETOM Sola system, while for the MAGNETOM Aera it was between 6 and 8 mm before the upgrade to syngo MRXA30 and in the same range as the MAGNETOM Sola after the upgrade. The average EPI ghosting ratio was (mean \pm σ) $2.3 \pm 0.2\%$ and $1.3 \pm 1.7\%$ for the MAGNETOM Sola and MAGNETOM Aera scanners respectively. Example results of the EPI long-term stability test are shown in Figure 7 for the Glover Stability QA protocol, and in Figure 8 for the Weisskoff analysis. The mean percent drift was (mean \pm σ) $0.10 \pm 0.09\%$ and $0.09 \pm 0.05\%$ while the mean percent fluctuation was (mean \pm σ) $0.038 \pm 0.005\%$ and $0.033 \pm 0.002\%$ for the MAGNETOM

Sola and MAGNETOM Aera scanners, respectively. In addition, the mean RDC was (mean \pm σ) 11.8 ± 1.9 and 14.7 ± 0.8 for the MAGNETOM Sola and MAGNETOM Aera scanner, respectively.

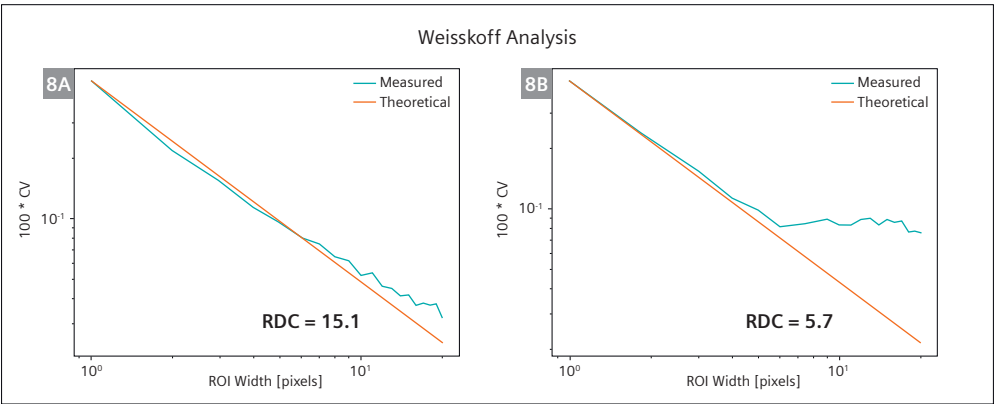
The parallel imaging SNR ratio stability is plotted in Figure 9 over a period of approximately four months for the five ROI locations previously shown in Figure 2. The average SNR ratio over the five locations is close to 1.41 ($\sqrt{2}$). Figure 10 shows the impact of the number of reference lines and calibration method on the SNR with GRAPPA, including the imaging time to incorporate a metric of efficiency. The results are showing a significant improvement in SNR and efficiency with the integrated calibration in comparison with the gradient echo separated calibration. There was 17% decrease in SNR between 24 integrated lines and 64-24 gradient echo configuration. The SNR improved with the number of reference lines with approximately 37% difference between 96 and 24 integrated lines.



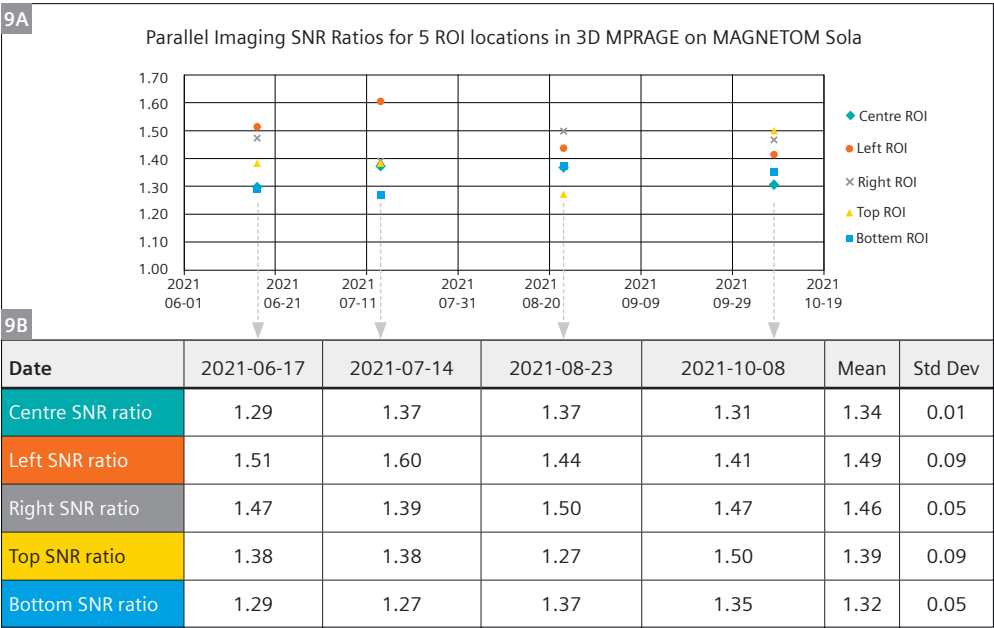
6 EPI distortion test showing (6A) the mask identified by the authors' analysis, (6B) EPI distortion data accumulated over 6 months for both MAGNETOM Sola and MAGNETOM Aera system.



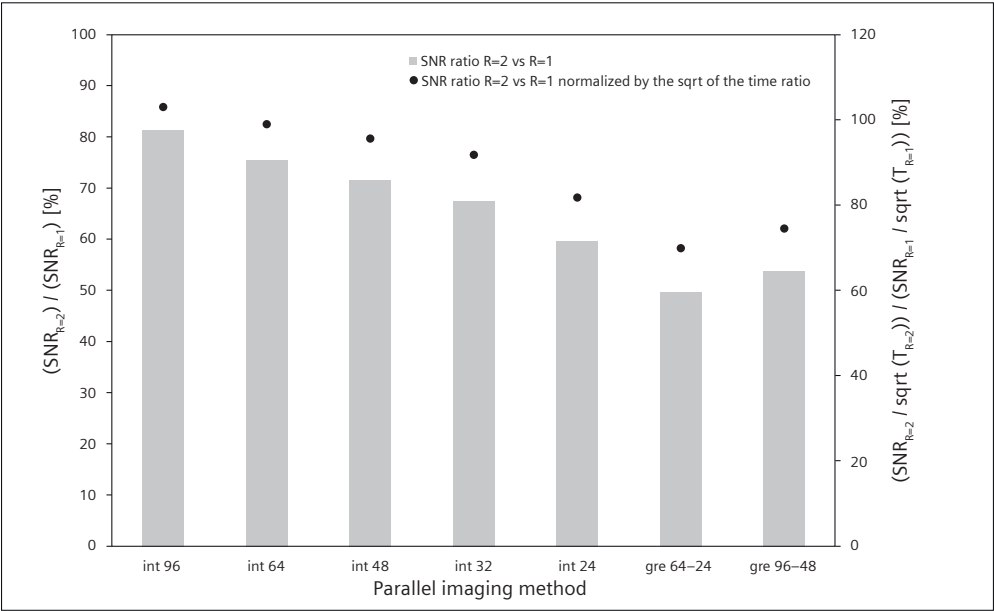
7 EPI stability test showing (7A) the signal drift over time (8 min 30 s), (7B) the noise magnitude spectrum from the accumulated data, (7C) the static noise as well as the even and odd data sum together, (7D) image of the first time-frame in combination with the corresponding polynomial fit of that data and the SFNR result.



8 Weisskoff analysis of an (8A) acceptable and (8B) unacceptable result.



9 Parallel imaging stability test showing (9A) a plot of SNR for the five identified regions of Figure 2 over a period of approximately 4 months and (9B) the table showing the mean and standard deviation over the five different regions.



Discussion

The complete end-to-end testing required by the AAPM task group reports [20–22] were performed without major issues. Investigation of the Body-30 receiver coil QA test showed a problem with the SNR reference values in version *syngo* MR XA20, the issue was rapidly resolved by Siemens Healthineers in subsequent version *syngo* MR XA31. Base-line data acquired with the coil was used as the reference while waiting for the bug fix, since the problem was detected during acceptance testing. Although the issue was not identified as major, it demonstrates the importance of testing coils as part of the acceptance testing as suggested by the different recommendations. The Siemens Healthineers service and clinical platforms [24] allowed us to cover most of AAPM recommended tests in a timely manner and would fit in a busy clinic, operating the machine 24 hours per day, 7 days per week. In addition to ease of use, the Siemens Healthineers service platform makes it straightforward for the MRI physicist to directly address any failing test or scanner issue with the technical support. A special attention should be given to shimming, particularly within the first 2 months of the magnet ramp-up. The gradient sensitivity was also an important check in our experience, as both machines needed to have their laser-to-isocentre distance re-adjusted (i.e., the programmed table motion that automatically brings the patient or phantom to isocentre after zeroing on the scanner's laser, which depends on the gradient sensitivity). Quality assurance and technical support are important in order to prevent issues and reach optimal scanner performance. For radiotherapy purposes, low-SAR RF pulses should be avoided in order to prevent thicker slices than expected (potentially biasing the MR-CT registration through-slice accuracy). Service key level 7 is needed in order to maintain a detailed record of the different QA results, which are in turn needed to identify trends and avoid exceeding action thresholds over time. The *syngo* MR XA31 software version on the MAGNETOM Sola and MAGNETOM Vida now allows the user to perform Phantom shim check, Gradient sensitivity check and synthesizer check on the customer platform without logging into service mode.

The geometric distortion characterization, performed over 90% of the usable FOV, showed that the vendor-implemented 3D correction algorithm mitigates, to a large extent, the geometric distortions on a sizable portion of the FOV (at least up to a 20 cm radius). The 3D-corrected average distortion is less than 1 mm within a 10 cm radius and less than 2 mm within a 25 cm radius around the isocenter on both the MAGNETOM Aera (Combi Dockable or standard table) and MAGNETOM Sola scanners. These

values are within the recommendation of the report 284 [22]. The measured distortion shows a clear downward trend on the MAGNETOM Sola compared to the MAGNETOM Aera; the average distortion on the MAGNETOM Sola is halved compared to the MAGNETOM Aera for radii of up to 20 cm and 50% less than the MAGNETOM Aera for radii of up to 25 cm. These values can be used as an estimate for the magnitude of system-related distortion on both the MAGNETOM Sola and MAGNETOM Aera platforms. Using a different distortion evaluation method may impact the results depending on the phantom field of view, number of data points and analysis method; however the repeatability and set-up sensitivity of the current method was validated in a previous study [26].

The superior B_0 homogeneity of the MAGNETOM Sola in comparison to the MAGNETOM Aera is clearly visible in Figure 5E and 5F and is confirmed by the histogram of the entire images in 5G. There is a significant difference between the histogram centers of approximately 0.1 ppm. In order to ensure a fair comparison, the same standard shimming routine was used on both systems. Therefore, the narrower full width at half maximum of the ΔB_0 histogram for the MAGNETOM Sola scanner is due to the superior intrinsic homogeneity of this magnet.

The EPI distortions on the MAGNETOM Aera scanner were reduced from 6.5 mm following the system installation with *syngo* MR E11E software to 2 mm after a system software upgrade (to version *syngo* MR XA30), which enabled using the exact same EPI sequence as on the MAGNETOM Sola scanner for comparison (version *syngo* MR XA20). The ACR phantom needs to be periodically refilled in order to avoid air bubbles at the surface (especially in the uniform slice of interest), as it could significantly increase the geometrical distortions locally, which could be responsible in part for the improvement seen after the upgrade. The ghosting ratio test is sensitive to the receiver coil arrangement and the image intensity correction filter. In fact, the intensity correction filter was found to be responsible for increasing the noise floor around the image as visible on the left-side/right-side of the phantom in Figure 1, consequently exaggerating the ghost ratio. Therefore, we deemed that either a moderate or no intensity correction is preferable for this QA test.

As demonstrated in Figure 7A the mean signal drift can be very minor on the Siemens Healthineers scanners tested in the current study and we did not observe a consistent tendency towards a positive drift as had been claimed previously [28]. Rather, the drift was occasionally positive and negative. The mean drifts reported in the current study for the MAGNETOM Sola and MAGNETOM Aera are significantly lower than those reported by Glover et al.

(0.3% at the lowest) [28], suggesting an interesting improvement in hardware stability since the early 2000s. The difference in average RDC is again attributed to different software versions (before the MAGNETOM Aera was upgraded to syngo MR XA30). Figure 8 shows a typical RDC in 8A and an abnormally low value in 8B. Glover et al. explain that a low RDC is often associated with a non-stationary and irregular time course of the residuals (after polynomial fit of the 150 dynamics).

In the parallel imaging stability test, an average SNR ratio over the five locations was found to be close to 1.41 ($= \sqrt{2}$), which is what one would expect in the case of a geometry factor (g factor) of 1. Normally, the geometry factor is greater than unity, but if a regularization is employed in the parallel imaging reconstruction, values below unity are possible [30, 31]. However, a desirable amount of regularization should approach a g factor of ~ 1 , which can be assumed when making SNR predictions on 3D MRI protocols with varying factors of acceleration [32]. In GRAPPA parallel imaging, the calibration method was shown to directly impact the SNR. In fact, the integrated method was shown to be significantly better in term of SNR with no significant difference in scan time compared to the GRE method. The SNR increases with the number of reference lines. A previous study recommended a minimum of 32 integrated lines to be used with GRAPPA [33]. The current study is in agreement with Blaimer et al. [33] and further suggests that 48 integrated lines better preserves SNR efficiency since the acquisition time is minimally impacted. High-resolution imaging is needed for radiotherapy planning, making it more difficult to preserve sufficient SNR in an acceptable scan time; therefore we recommend using 48 integrated lines with GRAPPA for these sequences.

Conclusion

The authors' experience showed no major problem during acceptance and commissioning. The Siemens Healthineers service platform was useful and time-saving in permitting medical physicists to perform most of the QA program in a semi-automatic or automatic fashion and in a clinically-acceptable time. The MAGNETOM Sola system was found to be more geometrically precise and accurate, with a more homogenous B_0 field making it suited for external-beam RT planning. Additional in-house tests allowed to track more advanced features and detected software upgrade changes. GRAPPA parallel imaging reference lines and calibration methods were optimized in order to obtain a sufficient SNR in a clinically-acceptable scan time for radiation therapy simulation.

References

- 1 Khoo VS, Joon DL. New developments in MRI for target volume delineation in radiotherapy. *Br J Radiol* 2006;79:S2–15.
- 2 Whitfield GA, Kennedy SR, Djoukharad IK, Jackson A. Imaging and target volume delineation in glioma. *Clin Oncol R Coll Radiol G B* 2014;26:364–76.
- 3 Schmidt MA, Payne GS. Radiotherapy planning using MRI. *Phys Med Biol* 2015;60:R323–61.
- 4 Haie-Meder C, Pötter R, Van Limbergen E, Briot E, De Brabandere M, Dimopoulos J, et al. Recommendations from Gynaecological (GYN) GEC-ESTRO Working Group (I): concepts and terms in 3D image based 3D treatment planning in cervix cancer brachytherapy with emphasis on MRI assessment of GTV and CTV. *Radiother Oncol* 2005;74:235–45.
- 5 Steenbakkers RJHM, Deurloo KEI, Nowak PJCM, Lebesque JV, van Herk M, Rasch CRN. Reduction of dose delivered to the rectum and bulb of the penis using MRI delineation for radiotherapy of the prostate. *Int J Radiat Oncol Biol Phys* 2003;57:1269–79.
- 6 Pötter R, Dimopoulos J, Georg P, Lang S, Waldhäusl C, Wachter-Gerstner N, et al. Clinical impact of MRI assisted dose volume adaptation and dose escalation in brachytherapy of locally advanced cervix cancer. *Radiother Oncol* 2007;83:148–55.
- 7 Owringi AM, Greer PB, Glide-Hurst CK. MRI-only treatment planning: benefits and challenges. *Phys Med Biol* 2018;63:05TR01.
- 8 Bauman G, Haider M, Van der Heide UA, Ménard C. Boosting imaging defined dominant prostatic tumors: A systematic review. *Radiother Oncol* 2013;107:274–81.
- 9 Monninkhof EM, Loon JWL van, Vulpen M van, Kerkmeijer LGW, Pos FJ, Haustermans K, et al. Standard whole prostate gland radiotherapy with and without lesion boost in prostate cancer: Toxicity in the FLAME randomized controlled trial. *Radiother Oncol* 2018;127:74–80.
- 10 Ulin K, Urie MM, Cherlow JM. Results of a multi-institutional benchmark test for cranial CT/MR image registration. *Int J Radiat Oncol Biol Phys* 2010;77:1584–9.
- 11 Korsager AS, Carl J, Riis Østergaard L. Comparison of manual and automatic MR-CT registration for radiotherapy of prostate cancer. *J Appl Clin Med Phys* 2016;17:294–303.
- 12 Brock KK, Deformable Registration Accuracy Consortium. Results of a multi-institution deformable registration accuracy study (MIDRAS). *Int J Radiat Oncol Biol Phys* 2010;76:583–96.
- 13 Pappas EP, Alshantqy M, Moutsatsos A, Lababidi H, Alsafi K, Georgiou K, et al. MRI-Related Geometric Distortions in Stereotactic Radiotherapy Treatment Planning: Evaluation and Dosimetric Impact. *Technol Cancer Res Treat* 2017;16:1120–9.
- 14 NessAiver M. Range of Results from over 534 ACR-mandated Annual MRI Performance Evaluations on over 204 Magnets from 8 Vendors Spanning a 10-year Period 2011. <http://www.simplyphysics.com/MRI%20QA%20RSNA%202011.pdf> (accessed September 21, 2021).
- 15 Weygand J, Fuller CD, Ibbott GS, Mohamed ASR, Ding Y, Yang J, et al. Spatial Precision in Magnetic Resonance Imaging-Guided Radiation Therapy: The Role of Geometric Distortion. *Int J Radiat Oncol* 2016;95:1304–16.
- 16 Poggi S, Pallotta S, Russo S, Gallina P, Torresin A, Bucciolini M. Neuronavigation accuracy dependence on CT and MR imaging parameters: a phantom-based study. *Phys Med Biol* 2003;48:2199–216.
- 17 Paulson ES, Erickson B, Schultz C, Allen Li X. Comprehensive MRI simulation methodology using a dedicated MRI scanner in radiation oncology for external beam radiation treatment planning. *Med Phys* 2015;42:28–39.

- 18 Price R, Allison J, Clarke G, Dennis M, Hendrick RE, Keener C, et al. 2015 Magnetic Resonance Imaging QUALITY CONTROL MANUAL 2015:126.
- 19 Glide-Hurst CK, Paulson ES, McGee K, Tyagi N, Hu Y, Balter J, et al. Task Group 284 Report: Magnetic Resonance Imaging Simulation in Radiotherapy: Considerations for Clinical Implementation, Optimization, and Quality Assurance. *Med Phys* n.d.;n/a.
- 20 Jackson E, Bronskill M, Drost D, Och J, Pooley R, Sobol W, et al. Acceptance Testing and Quality Assurance Procedures for Magnetic Resonance Imaging Facilities. AAPM; 2010.
- 21 Yanasak N, Clarke G, Stafford RJ, Goerner F, Steckner M, Bercha I, et al. Parallel Imaging in MRI: Technology, Applications, and Quality Control. AAPM; 2015.
- 22 Glide-Hurst CK, Paulson ES, McGee K, Tyagi N, Hu Y, Balter J, et al. Task group 284 report: magnetic resonance imaging simulation in radiotherapy: considerations for clinical implementation, optimization, and quality assurance. *Med Phys* 2021;48:e636–70.
- 23 Zhang B, Stanescu T, Wachowicz K, King J, Côté J-C. Canadian Partnership for Quality Radiotherapy Technical Quality Control Guidelines for Magnetic Resonance Imaging for Radiation Treatment Planning 2020. https://www.cpqr.ca/wp-content/uploads/2020/09/MRI-2020-09-01_FR.pdf (accessed November 30, 2021).
- 24 Siemens Healthineers. Commissioning and Quality Assurance (QA) for MAGNETOM systems in radiation therapy n.d. https://cdn0.scrvt.com/39b415fb07de4d9656c7b516d8e2d907/73afee707dbc96c2/8490b30ac680/MR_Quality_Assurance_Guide_for_MR_in_RT_FINAL.pdf (accessed November 11, 2021).
- 25 Gustafsson C, Nordström F, Persson E, Brynolfsson J, Olsson LE. Assessment of dosimetric impact of system specific geometric distortion in an MRI only based radiotherapy workflow for prostate. *Phys Med Biol* 2017;62:2976–89.
- 26 Wyatt J, Hedley S, Johnstone E, Speight R, Kelly C, Henry A, et al. Evaluating the repeatability and set-up sensitivity of a large field of view distortion phantom and software for magnetic resonance-only radiotherapy. *Phys Imaging Radiat Oncol* 2018;6:31–8.
- 27 Angers C, Bottema R, Buckley L, Studinski R, Petzold D, Abbassian F, et al. Streamlining Regulatory Activities Within Radiation Therapy Departments Using QATrack+. *Health Phys* 2019;117:306–312.
- 28 Friedman L, Glover GH. Report on a multicenter fMRI quality assurance protocol. *J Magn Reson Imaging* 2006;23:827–39.
- 29 Weisskoff RM. Simple measurement of scanner stability for functional NMR imaging of activation in the brain. *Magn Reson Med* 1996;36:643–5.
- 30 Lin F-H. Prior-Regularized GRAPPA Reconstruction. *Proc Intl Soc Magn Reson Med* 2006;14:3656.
- 31 Lin F-H, Kwong KK, Belliveau JW, Wald LL. Parallel imaging reconstruction using automatic regularization. *Magn Reson Med* 2004;51:559–67.
- 32 Jutras J-D, Wachowicz K, Gilbert G, De Zanche N. SNR efficiency of combined bipolar gradient echoes: Comparison of three-dimensional FLASH, MPRAGE, and multiparameter mapping with VFA-FLASH and MP2RAGE. *Magn Reson Med* 2017;77:2186–202.
- 33 Blaimer M, Breuer FA, Mueller M, Seiberlich N, Ebel D, Heidemann RM, et al. 2D-GRAPPA-operator for faster 3D parallel MRI. *Magn Reson Med* 2006;56:1359–64.

Contact

Professeur associé Éric Poulin
 Département de radio-oncologie et
 Axe Oncologie du Centre de recherche
 du CHU de Québec
 CHU de Québec-Université Laval
 Centre intégré de cancérologie
 2250, boulevard Henri-Bourassa
 Québec, QC, G1G 5X1
 Canada
 Eric.poulin@chudequebec.ca



